

AD-A275 890



12

Wall Pressure Events From the Direct Numerical Simulation of A Turbulent Wall-Bounded Flow

Submarine Sonar Department

Richard M. Lueptow
Northwestern University

DTIC
ELECTE
FEB 17, 1994
S B D

DTIC QUALITY INSPECTED 2



424
487

94-05138



Naval Undersea Warfare Center Detachment
New London, Connecticut

Approved for public release; distribution is unlimited.

94 2 16 007

PREFACE

This report was prepared under Project No. M63000, *Multimode Directional Towed Arrays*, principal investigator M. J. Berliner, Code 2141, NUWC Detachment New London. The sponsoring activity was the Office of Naval Research, T. G. Goldsberry, Code 451.

The technical reviewer for this report was W. L. Keith (Code 2141), NUWC Detachment New London.

REVIEWED AND APPROVED: 6 DECEMBER 1993


F. J. Kingsbury
Head, Submarine Sonar Department

REPORT DOCUMENTATION PAGE			Form Approved OMB No. 0704-0188	
<small>Public reporting burden for this collection of information is estimated to average 1 hour per response, including the time for reviewing instructions, searching existing data sources, gathering and maintaining the data needed, and completing and reviewing the collection of information. Send comments regarding this burden estimate or any other aspect of this collection of information, including suggestions for reducing this burden, to Washington Headquarters Services, Directorate for Information Operations and Reports, 1215 Jefferson Davis Highway, Suite 1204, Arlington, VA 22202-4302, and to the Office of Management and Budget, Paperwork Reduction Project (0704-0188), Washington, DC 20503.</small>				
1. AGENCY USE ONLY (Leave Blank)	2. REPORT DATE 6 December 1993	3. REPORT TYPE AND DATES COVERED FINAL		
4. TITLE AND SUBTITLE Wall Pressure Events From the Direct Numerical Simulation of a Turbulent Wall-Bounded Flow		5. FUNDING NUMBERS RJ14A61		
6. AUTHOR(S) Submarine Sonar Department and Richard M. Lueptow, Northwestern University				
7. PERFORMING ORGANIZATION NAME(S) AND ADDRESS(ES) Naval Undersea Warfare Center Detachment New London New London, Connecticut 06320		8. PERFORMING ORGANIZATION REPORT NUMBER TR 10,481		
9. SPONSORING/MONITORING AGENCY NAME(S) AND ADDRESS(ES) Office of Naval Research 800 North Quincy St. Alexandria, VA 22217-5000		10. SPONSORING/MONITORING AGENCY REPORT NUMBER		
11. SUPPLEMENTARY NOTES				
12a. DISTRIBUTION/AVAILABILITY STATEMENT Approved for public release; distribution is unlimited.		12b. DISTRIBUTION CODE		
13. ABSTRACT (Maximum 200 words) Wall pressure events beneath a turbulent wall-bounded flow are related to turbulence-generating events in the flow. The data base for a direct numerical simulation of channel flow allows the analysis of significant pressure events in space and time. Both positive and negative wall pressure events in the data base were detected with a pressure peak conditional sampling technique. The recovered events were ensemble averaged to provide a space and time record of a typical event. Both positive and negative pressure peak events have regions of pressure of the opposite sign just ahead of and just behind them, but the regions of opposite sign do not extend to the sides of the events. Although a positive pressure peak event begins as a double positive pressure hump, the downstream hump eventually dominates and becomes the pressure peak before the event decays. Negative pressure peak events begin as a positive hump leading a negative hump. The negative hump grows to become the peak before decaying. Both positive and negative events begin about 400 wall units upstream of where the maximum pressure occurs and persist to about 400 wall units downstream of the pressure peak. The entire event lasts about $0.4 \delta/U_\tau$.				
14. SUBJECT TERMS Direct Numerical Simulation, Pressure Peak, Turbulent Boundary Layer, Wall Pressure		15. NUMBER OF PAGES 22		
		16. PRICE CODE		
17. SECURITY CLASSIFICATION OF REPORT UNCLASSIFIED	18. SECURITY CLASSIFICATION OF THIS PAGE UNCLASSIFIED	19. SECURITY CLASSIFICATION OF ABSTRACT UNCLASSIFIED	20. LIMITATION OF ABSTRACT SAR	

TABLE OF CONTENTS

	Page
INTRODUCTION	1
NUMERICAL DATA BASE.....	2
RESULTS	3
CONCLUSIONS.....	11
REFERENCES.....	13

LIST OF ILLUSTRATIONS

Figure		Page
1	Contours of Wall Pressure at a Typical Instant in Time	4
2	Translation of Wall Pressure Events Over a Period of Time of 0.375 δ/U_τ	5
3	Ensemble Average of Conditionally Sampled Positive Pressure Peak Events	7
4	Ensemble Average of Conditionally Sampled Negative Pressure Peak Events	9
5	Ensemble Average of the Time Development of Conditionally Sampled Pressure Peak Events Exceeding ± 4 p _{rms}	10

LIST OF TABLES

Table		Page
1	Parameters of the Direct Simulation Data Base	2

Accession For	
NTIS GRA&I	<input checked="" type="checkbox"/>
DTIC TAB	<input type="checkbox"/>
Unannounced	<input type="checkbox"/>
Justification	
By	
Distribution/	
Availability Codes	
Dist	Avail and/or Special
A-1	

i/ii
Reverse Blank

WALL PRESSURE EVENTS FROM THE DIRECT NUMERICAL SIMULATION OF A TURBULENT WALL-BOUNDED FLOW

INTRODUCTION

Although wall pressure events beneath a turbulent boundary layer have been experimentally detected with pressure transducers mounted in the wall, the number of spatial locations at which the wall pressure can be measured is limited. The wall pressure frequency spectrum or wall pressure events, such as pressure peaks, can, however, be measured at a handful of locations as a function of time, although the character of the pressure field in space cannot be determined from these measurements at a few discrete locations. On the other hand, direct numerical simulation of turbulent wall-bounded flow offers access to the wall pressure field across an entire region of the flow, permitting the calculation of the wavenumber spectrum and the detection of wall pressure events in space. Unfortunately, the nature of direct numerical simulations is such that the Reynolds number is artificially low and the duration of time of the simulation is severely limited. Nevertheless, wall pressure data from direct numerical simulation of a turbulent channel flow provide a spatial representation of a turbulent field that is otherwise unattainable.

Conditional sampling of experimental wall pressure data has been used to characterize significant pressure "events" related to the turbulent velocity field. Typically, the wall pressure and the velocity are measured simultaneously at discrete locations in the flow, and events are detected with a variety of techniques. Use of this process in a planar boundary layer has allowed positive peaks in the wall pressure to be correlated with streamwise acceleration related to near-wall shear layers.¹⁻⁴ Since such shear layers are closely related to turbulence generation mechanisms near the wall, these measurements indicate that positive wall pressure peaks are coupled with turbulence production. Apart from conditionally sampled events, though, positive wall pressures generally are associated with high streamwise velocity, and negative pressures are associated with low streamwise velocity.² In a boundary layer on a cylinder, large-amplitude negative pressure peaks have been associated with local decreases in streamwise velocity, indicating a bidirectional relationship or coupling between large-amplitude wall pressure fluctuations and the rate of change of streamwise velocity near the wall.⁵

Results are reported here for the detection of wall pressure events in the National Aeronautics and Space Administration/Ames Flight Center (NASA-Ames) direct numerical simulation data base of turbulent channel flow. The goal of the work was to characterize the nature of pressure

peak events in the spatial domain. Unfortunately, velocity data are not available for this data base, and so the velocity field and the pressure at the wall cannot be related to one another as in the studies described in references 1 through 5. In spite of this shortcoming, the numerical data base provides information on the spatial character of wall pressure events that cannot be obtained from experiments with transducers at a limited number of points.¹⁻⁵ In the work presented here, the development of wall pressure events in both time and space is investigated. The results help provide an understanding of the turbulent nature of the wall pressure fields in wall-bounded turbulent flow.

NUMERICAL DATA BASE

A direct numerical simulation of turbulent channel flow, described in detail by Kim et al.,⁶ was used to generate the pressure statistics presented in this report. This data base is the same as that used by Kim⁷ and by Choi and Moin⁸ for analysis of the structure and space-time characteristics of turbulent wall pressure fluctuations. The computational domain for the simulation is $L_x \times L_y \times L_z$ of $4\pi\delta \times 2\delta \times (4\pi/3)\delta$ in the streamwise x , wall-normal y , and spanwise z directions, where δ is the half-channel width. The number of grid points N and other details of the computational domain and flow parameters are provided in table 1. The simulation was carried out for 25,640 time steps, saving the pressure for the entire plane of one of the walls at every tenth step corresponding to $\Delta t = 3.75 \times 10^{-3} \delta/U_\tau$. The data base was stored in MATLAB-compatible format on a Sun workstation after translation from the original Cray-compatible storage format. The results described here are based on the first 1500 time steps, corresponding to a total time of $5.625 \delta/U_\tau$.

Table 1. Parameters of the Direct Simulation Data Base⁶

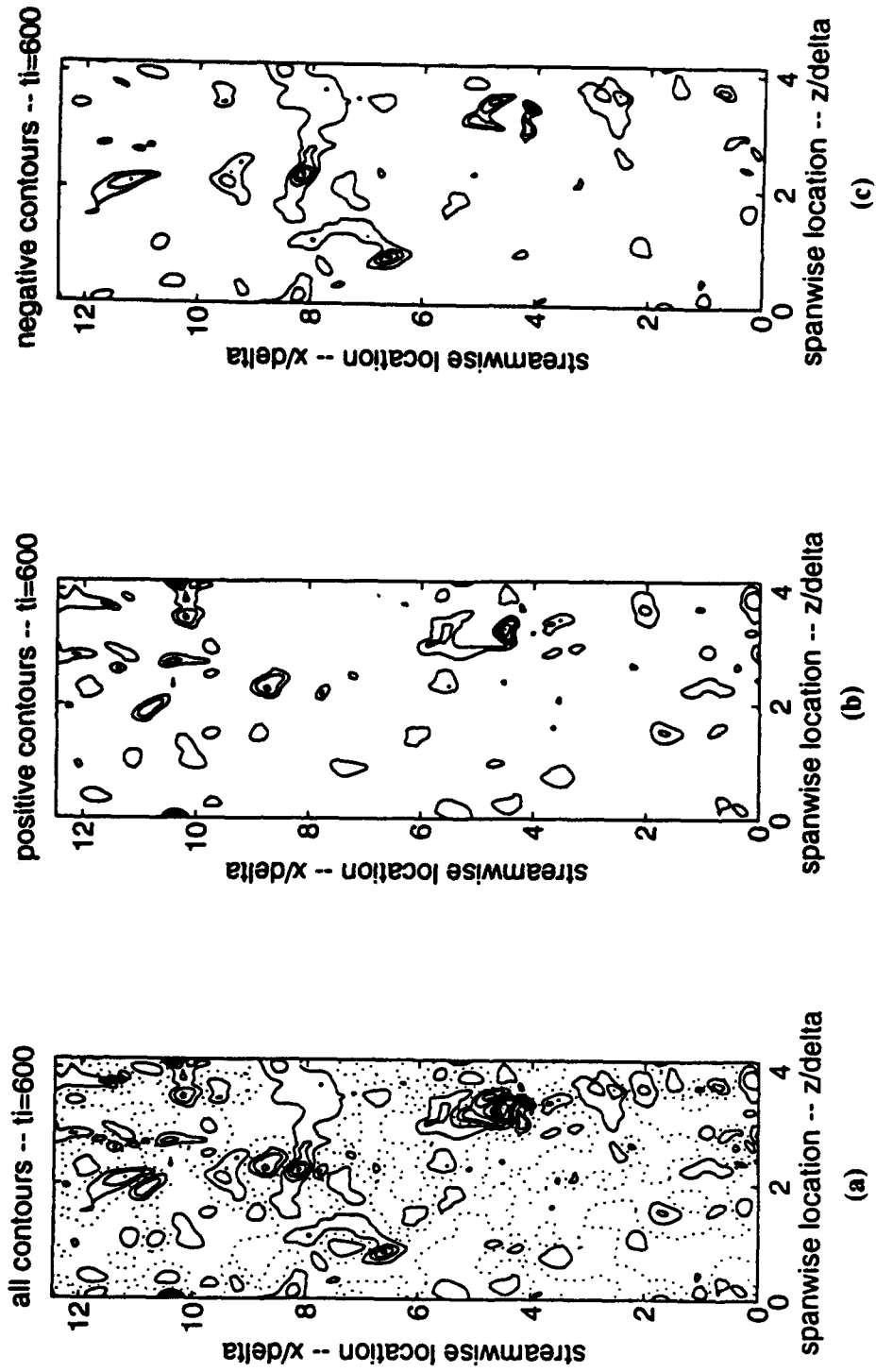
$Re_\delta = U_{cl}\delta/\nu = 3200$							
$Re_\theta = U_{cl}\theta/\nu = 280$							
$Re_\tau = U_\tau\delta/\nu = 180$							
Streamwise:	$L_x/\delta = 4\pi$	$N_x = 128$	$\Delta x_+ = 17.6$	$L_{x+} = 2253$			
Wall-normal:	$L_y/\delta = 2$	$N_y = 129$	$\Delta y_+ = 0.05$ (near wall) to				
			$\Delta y_+ = 4.4$ (centerline)				
Spanwise:	$L_z/\delta = 4\pi/3$	$N_z = 128$	$\Delta z_+ = 5.9$	$L_{z+} = 755$			
			$\Delta t U_\tau/\delta = 3.75 \times 10^{-3}$				

Although this numerical data base provides a vast set of wall pressure data, there are several drawbacks. First, the momentum thickness Reynolds number for the simulation, $Re_\theta = 280$, is probably physically unrealizable, although the low Reynolds number is necessary because of computational limitations. Second, periodic boundary conditions require that the fluid structures entering the computational domain be identical to those leaving the domain, which cannot occur in a real channel flow. Third, the extent of the computational domain is very limited, 2253 viscous units in the streamwise direction and 755 viscous units in the spanwise direction. Fourth, the wavenumber spectrum of the wall pressure has a suspicious increase in energy as the wavenumber approaches zero.⁹ Finally, the position of the centerline of the simulated channel is at a very small distance from the wall corresponding to $\delta U_\tau/\nu=180$, which suggests that contributions by the inner region of the flow may dominate because the outer flow is largely absent.

RESULTS

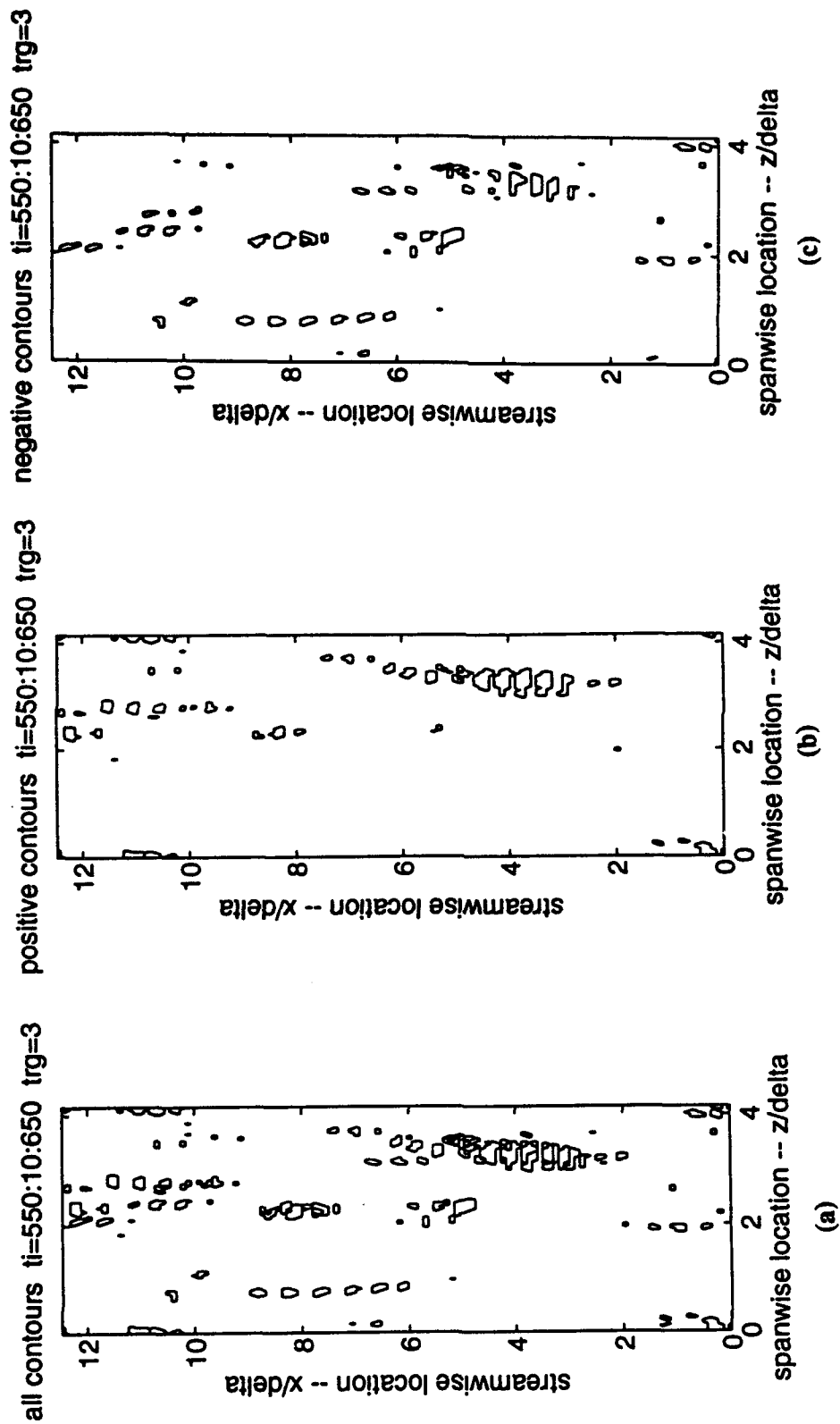
A contour plot of the wall pressure at a typical instant in time is shown in figure 1a. Given the spacing for the contours of $1 p_{rms}$, it is evident that most of the field has relatively low levels of pressure fluctuations. Only within the solid contours does the wall pressure exceed $\pm 1 p_{rms}$. The positive and negative contours for $p > p_{rms}$ are shown in figures 1b and 1c, respectively. Both positive and negative contours are each fairly uniformly distributed in space and seem to have no preferential elongation or shape. But positive and negative pressure regions seem to often be located near one another (for instance, at $z/\delta \sim 3$ and $x/\delta \sim 5$).

Relatively strong pressure events are tracked in time in figure 2a. In this figure, events exceeding $\pm 3 p_{rms}$ are tracked for a time period of $0.375 \delta/U_\tau$ and plotted every $0.0375 \delta/U_\tau$. A series of similarly sized contours in a vertical line shows the motion of the pressure event. For instance, at $z/\delta \sim 1$, the line of contours extending from $x/\delta \sim 9$ to 6 shows the translation of a negative pressure event moving from top to bottom in the domain. A typical strong pressure event is evident at $z/\delta \sim 3$ and $x/\delta \sim 2$ to 6. The streamwise extent of the event is several δ , and the duration of the event is at least as long as the time covered in the figure, which is $0.375 \delta/U_\tau$. Positive and negative events are shown in figures 2b and 2c, respectively, where it is evident that such events often occur near one another (for instance, at $z/\delta \sim 3$ and $x/\delta \sim 2$ to 6). On the other hand, positive and negative events do not necessarily occur near one another (for instance, a negative event at $z/\delta \sim 1$ and $x/\delta \sim 6$ to 9).



Flow is from top to bottom. Dotted curves are zero pressure contours. Solid curves are nonzero contours spaced at $1 p_{rms}$.

Figure 1. Contours of Wall Pressure at a Typical Instant in Time



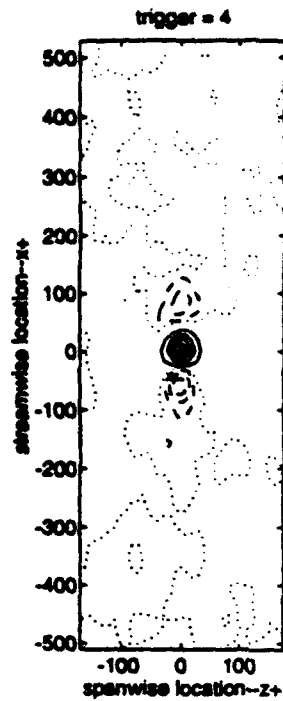
*Contour lines are shown at increments of $0.0375 \delta U_\tau$ for wall pressures exceeding $\pm 3 p_{rms}$.
Flow is from top to bottom*

Figure 2. Translation of Wall Pressure Events Over a Period of Time of $0.375 \delta U_\tau$

Substantial information regarding the character of significant wall pressure events can be obtained from the analysis of "typical" ones. To accomplish this, pressure peaks exceeding a trigger level, $k p_{rms}$, were ensemble averaged to generate a typical event. A similar technique is used in analyzing the wall pressure time signature obtained from experimental wall pressure measurements.^{1,2} However, the numerical simulation data base permits the detection of pressure peak events in both space and time. The detection begins with a search for peaks exceeding the trigger level for a single instant. After all the peaks have been found for that time instant, the next time instant is searched for peaks exceeding the threshold. Of course, most peaks found at the first time instant are also found at the second time instant. Each peak is compared to the peaks found at the previous time instant to determine which peak is larger. Subsequent time instants are searched for peaks and checked against nearby peaks from previous time instants. As this process continues, the location and time instant corresponding to the maximum for each pressure peak exceeding the trigger are found. After locating all pressure peak events in the data base, the pressure field surrounding each detected event is recovered from the data base and ensemble averaged with other events to create the pressure field surrounding a typical event.

The results of such an analysis for positive pressure events are shown in figure 3. Pressure contours of a positive event for $k = 4$ are shown in figure 3a. The pressure event has been centered in the figure at the origin. Although most of the surrounding pressure field has been averaged out to nearly zero pressure, just upstream and downstream of the positive pressure event, negative pressure occurs. The negative pressure area is relatively weak compared with the positive pressure event. The negative pressure area does not extend to the side of the pressure peak.

Slices through the positive pressure event in the streamwise and spanwise directions are shown in figures 3b and 3c, respectively, for five trigger levels. Of course, the height of the peak varies with the trigger level. The negative pressure just upstream and downstream of the pressure peak is evident in figure 3b. The upstream negative pressure area is dependent upon the trigger level. Stronger positive pressure peaks result in stronger negative pressures upstream of, or behind, the peak. The downstream negative pressure region is weaker and somewhat less dependent upon trigger level. The pressure peak itself has a streamwise and spanwise extent of about 80 wall units. The negative pressure ahead of the pressure peak extends 80 to 150 wall units downstream, and the negative pressure behind it extends about 50 wall units upstream. Similar results are evident in the ensemble-averaged pressure for Variable Interval Space Averaging (VISA) events detected based on the streamwise velocity.³ The authors used the



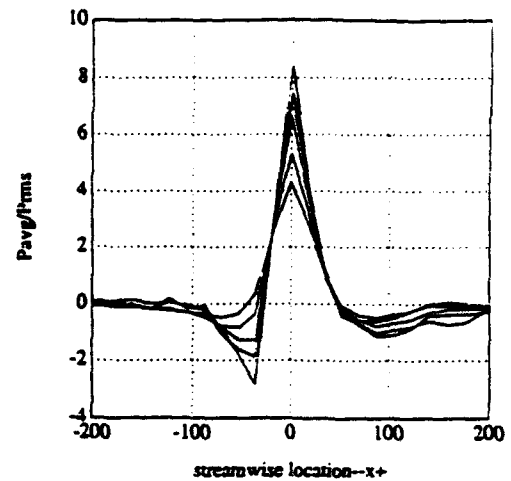
(a)

← Contour Plot of a Typical Event Exceeding 4 prms
(Based on 194 Individual Events)

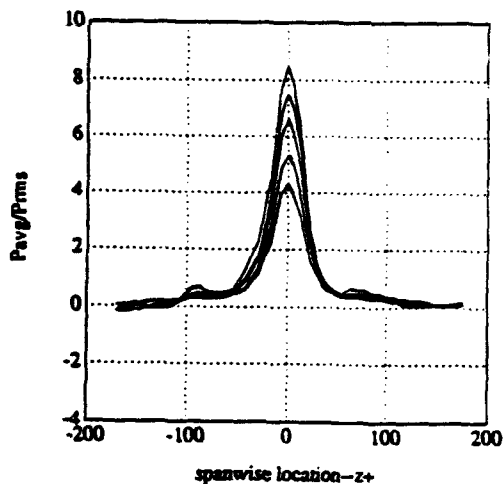
Dotted curves are zero pressure contours. Solid curves are positive contours spaced at 1 prms. Dashed curves are negative contours spaced at 0.25 prms. Positive pressure peak is centered at the origin. Upstream corresponds to negative x, and downstream corresponds to positive x.

Cut Through the Contours Along a Streamwise Line Through the Pressure Maximum →

Trigger levels of 3, 4, 5, 6, and 7 prms are identifiable by the height of the pressure peak (largest trigger levels are highest).



(b)



(c)

← Cut Through the Contours Along a Spanwise Line Through the Pressure Maximum

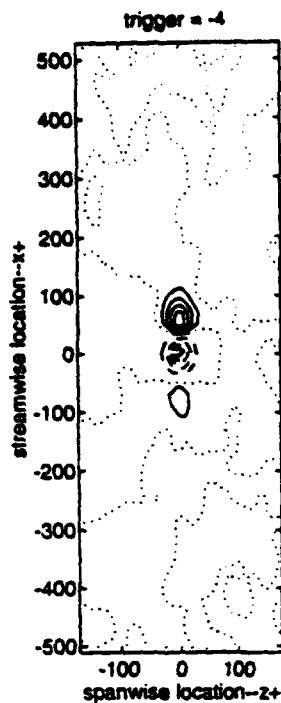
Figure 3. Ensemble Average of Conditionally Sampled Positive Pressure Peak Events

same data base, but only peripherally considered the pressure at the wall. Nevertheless, they showed that a positive peak in pressure is related to a shear layer directly above the location of the maximum pressure. The shear layer is similar to positive events detected experimentally with Variable Interval Time Averaging (VITA). Johansson et al.³ also show contours of pressure at $y^+ = 15$, corresponding to a VISA-detected shear layer. The negative contours at this distance from the wall differ considerably from those at the wall shown in figure 3a. In addition to regions of negative pressure ahead of and behind the pressure event, the negative contours extend along either side of the pressure peak.

A similar analysis of negative wall pressure events is shown in figure 4. The negative pressure peak, centered at the origin in figure 4a, lies between weak positive pressure regions upstream and downstream of the event. The strength of the positive pressure area is dependent upon the threshold, as indicated in figure 4b. Higher thresholds result in a higher positive pressure, especially ahead of the event. The negative pressure events are not as broad as positive events (see figure 4c).

The time history of ensemble-averaged positive wall pressure events is shown in figure 5a for a threshold of $k = +4$. Each curve is the wall pressure at an instant in time along a streamwise line aligned with the spanwise center of the pressure maximum. No wall pressure peak is evident in the lowest curve for a time of $-0.225 \delta/U_\tau$, but by the next time instant, two small bumps appear at $x^+ = -500$. As time progresses, the upstream bump grows larger than the downstream bump (at $-0.15 \delta/U_\tau$ and $-0.1125 \delta/U_\tau$). Then the downstream bump grows much larger (at $-0.075 \delta/U_\tau$ and $-0.0375 \delta/U_\tau$), eventually becoming the pressure peak. The decay of the pressure peak shows some hint of the double pressure peak again (at $0.1125 \delta/U_\tau$ and $0.1875 \delta/U_\tau$). The pressure peak broadens as it decays. Similar results occur for trigger levels of $k = 3, 5, 6$, and 7 . Since positive pressure peaks have been associated with shear layers that are related to the bursting process,¹⁻⁴ it is reasonable to assume that the double bump leading to the pressure peak is also related to this process. However, it is difficult to relate the double bump to common conceptual models of the process leading to a burst, such as a hairpin vortex.

The time history for a negative event is shown in figure 5b. In this case, the negative bump leading to the peak is preceded by a slight positive pressure ($-0.1125 \delta/U_\tau$ through $-0.0375 \delta/U_\tau$). This leading positive pressure becomes the relatively strong positive pressure ahead of the negative pressure peak. After the negative peak, the pressure peak broadens and decays. Negative pressure peaks have been related to decelerations of the streamwise velocity.⁵ But it is unclear if negative pressure peaks can be related to any coherent turbulence generation process in



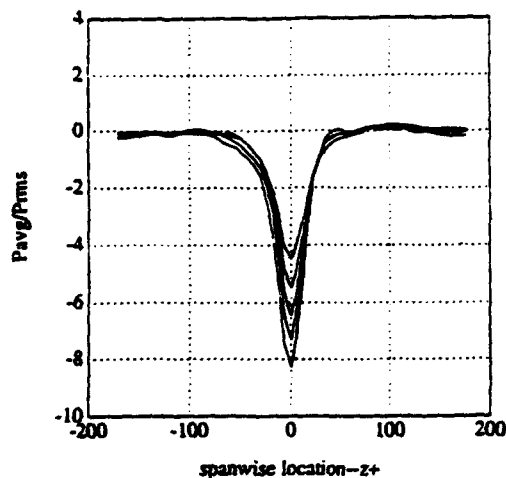
← Contour Plot of a Typical Event Exceeding -4 prms
(Based on 230 Individual Events)

Dotted curves are zero pressure contours. Solid curves are positive contours spaced at 0.25 prms . Dashed curves are negative contours spaced at 1 prms . Negative pressure peak is centered at the origin. Upstream corresponds to negative x , and downstream corresponds to positive x .

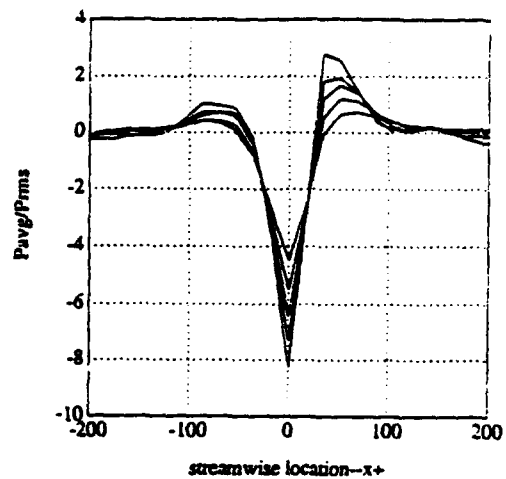
(a)

Cut Through the Contours Along a Streamwise Line Through the Pressure Minimum →

Trigger levels of -3 , -4 , -5 , -6 , and -7 prms are identifiable by the height of the pressure peak (largest trigger levels are highest).



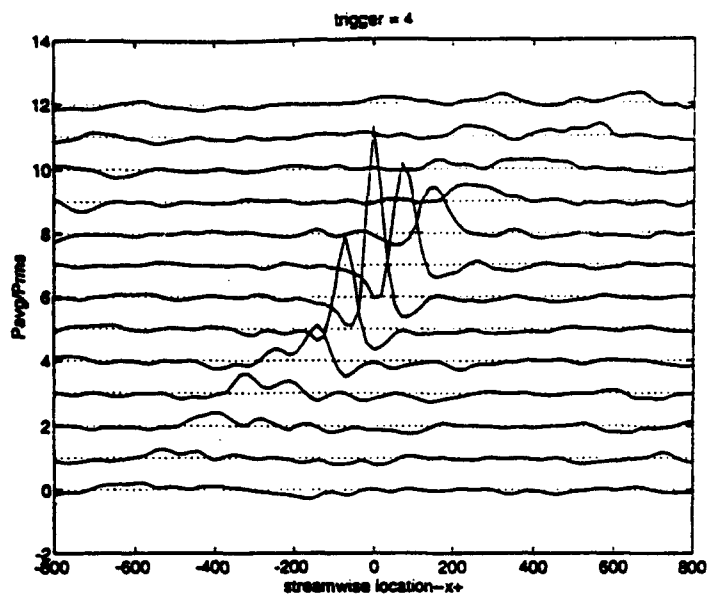
(c)



(b)

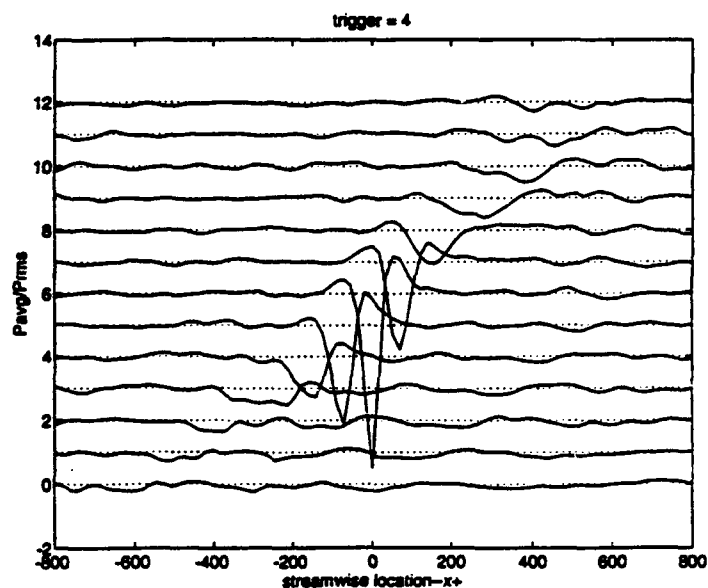
← Cut Through the Contours Along a Spanwise Line Through the Pressure Minimum.

Figure 4. Ensemble Average of Conditionally Sampled Negative Pressure Peak Events



← Positive Event

(a)



Negative event →

(b)

Each curve is a cut along a streamwise line through the pressure peak. Time progresses from the bottom curve to the top curve. The time step between curves is $0.0375 \delta U \tau$ (curves correspond to $-0.225, -0.1875, -0.15, -0.1125, -0.075, -0.0375, 0, 0.0375, 0.075, 0.1125, 0.15, 0.1875, 0.225$ from bottom to top). The time for which the pressure peak occurs is the seventh curve from the bottom. Flow is from left to right.

Figure 5. Ensemble Average of the Time Development of Conditionally Sampled Pressure Peak Events Exceeding ± 4 prms

the boundary layer in the same way that positive pressure peaks have been related to the bursting process.

CONCLUSIONS

By following wall pressure events in both space and time, certain characteristics of the evolution of these events have been found. Positive and negative events often appear in the same localized region of the flow. Ensemble averages of conditionally sampled pressure peak events show that a negative pressure appears ahead of and behind a positive pressure peak, although not at the sides of the pressure peak. Similarly, a positive pressure appears ahead of and behind a negative pressure peak, but not at its sides. Positive pressure peaks have been associated with the shear layer related to bursting. Based on the results of Johansson et al.,³ the streamwise velocity is negative and the wall-normal velocity is positive above the negative pressure that is ahead of the pressure peak, and vice versa for the negative pressure behind the pressure peak. As a result, the small negative pressures ahead of and behind the positive pressure peak are related to high levels of Reynolds-stress-associated production.³

The relation between negative pressure peaks and flow structures has not been discussed to any extent in the literature. Nevertheless, negative pressure peaks contribute as much to the wall pressure spectrum as do positive pressure peaks, are as energetic as positive pressure peaks, and occur as frequently as positive pressure peaks. Consequently, a full understanding of the wall pressure requires further knowledge of how flow structures are related to negative pressure peaks.

The sequence of events leading to positive pressure peaks includes the appearance of a double positive pressure hump before the maximum pressure. Eventually, the downstream hump becomes the dominant pressure peak, which then decays as it moves downstream. Without further analysis, it is unclear how the double hump leading to the pressure maximum is related to commonly hypothesized structures and events in the flow. The pressure signature leading to a negative pressure peak consists of a negative hump behind a positive hump. The negative hump grows substantially, becomes the pressure peak, and then decays. Again it is difficult to relate the development of the flow structure to a flow structure in the boundary layer.

REFERENCES

1. A. V. Johansson, J. Her, and J. H. Haritonidis, "On the Generation of High-Amplitude Wall-Pressure Peaks in Turbulent Boundary Layers and Spots," *Journal of Fluid Mechanics*, vol. 175, 1987, pp. 119-142.
2. J. H. Haritonidis, L. S. Gresko, and K. S. Breuer, "Wall Pressure Peaks and Waves," in *Near-Wall Turbulence: Proceedings of the 1988 Zoran Zaric Memorial Conference.*, eds. S. J. Kline and N. H. Afgan, Hemisphere Publishing Co., 1990, pp. 397-417.
3. A. V. Johansson, P. H. Alfredsson, and J. Kim, "Evolution and Dynamics of Shear-Layer Structures in Near-Wall Turbulence," *Journal of Fluid Mechanics*, vol. 224, 1991, pp. 579-599.
4. J. A. Astolfi, P. Bally, A. Fages, and B. E. Forestier, "Relation Between Wall-Pressure Fluctuations and a Large Instantaneous Velocity Gradient $\partial U/\partial y$ Beneath a Turbulent Boundary Layer," *European Journal of Mechanics, B/Fluids*, vol. 11, 1992, pp. 573-586.
5. S. R. Snarski and R. M. Lueptow, "Wall Pressure and Turbulent Structures in a Turbulent Boundary Layer on a Cylinder in Axial Flow" submitted to *Journal of Fluid Mechanics*, 1993.
6. J. Kim, P. Moin, and R. Moser, "Turbulence Statistics in Fully Developed Channel Flow at Low Reynolds Number," *Journal of Fluid Mechanics*, vol. 177, 1987, pp. 133-166.
7. J. Kim, "On the Structure of Pressure Fluctuations in Simulated Turbulent Channel Flow," *Journal of Fluid Mechanics*, vol. 205, 1989, pp. 421-451.
8. H. Choi and P. Moin, "On the Space-Time Characteristics of Wall-Pressure Fluctuations," *Physics of Fluids, A2*, 1990, pp. 1450-1460.
9. Personal communication with W. L. Keith and B. Abraham, Naval Undersea Warfare Center, New London, CT, 1993.

INITIAL DISTRIBUTION LIST

Addressee	No. of Copies
DTIC	12
NORTHWESTERN UNIV [R. Lueptow]	15